coatings

MDPI

Article

Effect of Microcapsule Concentration with Different Core-Shell Ratios on Waterborne Topcoat Film Properties for *Tilia europaea*

Xiaoxing Yan [1,2,*], Wenting Zhao [2], Lin Wang [2] and Xingyu Qian [2]

[1] Co-Innovation Center of Efficient Processing and Utilization of Forest Resources, Nanjing Forestry University, Nanjing 210037, China

[2] College of Furnishings and Industrial Design, Nanjing Forestry University, Nanjing 210037, China; zhaowenting@njfu.edu.cn (W.Z.); wanglin@njfu.edu.cn (L.W.); qianxingyu@njfu.edu.cn (X.Q.)

* Correspondence: yanxiaoxing@njfu.edu.cn

Abstract: The effects of the core-shell ratio and concentration of urea formaldehyde (UF) resin-coated waterborne acrylic resin microcapsules on the optical properties, mechanical properties and liquid resistance of waterborne topcoat coatings on the surface of *Tilia europaea* were investigated. With the increase of microcapsule concentration, the color difference and hardness of the paint film gradually increased, the gloss and adhesion of the paint film gradually decreased, and the impact resistance and elongation at break of the paint film increased first and then decreased. With the increase of the core-shell ratio, the hardness and impact resistance of the paint film increased first and then decreased, and the adhesion of the paint film decreased gradually. Red ink had a great influence on the liquid resistance of paint film. When the core-shell ratio of UF-coated waterborne acrylic resin microcapsule was 0.58:1 and the microcapsule concentration was 10.0%, the comprehensive performance of paint film on *Tilia europaea* was better. The prepared self-healing microcapsules applied to the waterborne coatings committed to prolonging the service life of the paint film.

Keywords: microcapsule; core-shell ratio; waterborne topcoat

check for updates

Citation: Yan, X.; Zhao, W.; Wang, L.; Qian, X. Effect of Microcapsule Concentration with Different Core-Shell Ratios on Waterborne Topcoat Film Properties for *Tilia europaea*. *Coatings* **2021**, *11*, 1013. https://doi.org/10.3390/coatings11091013

Academic Editor: Joseph L. Keddie

Received: 26 July 2021
Accepted: 22 August 2021
Published: 24 August 2021

1. Introduction

As a natural polymer composite material, wood material has unique texture and color [1]. It is a common green resource in nature [2]. As environmental awareness is growing, wood materials have become the preferred object of use because of their high strength to weight ratio, low energy consumption, natural degradation and recyclable utilization, and they are widely used in construction, indoor, packaging, railway transportation (as hardwood sleepers) and other production activities [3,4]. However, the cellulose, the main component of such kind of materials, contains many hydrophilic groups, which leads to its wet expansion and the drying of the wood, with a size variation which limits its application scopes and further affects its service life [5–8]. In general, wood materials are subjected to surface treatments before being put into actual use [9–13]. The rheology and stabilizers are very important for the properties of coatings [14]. Waterborne wood coatings are very popular in wood surface finishing because of their advantages regarding environmental protection, pollution resistance and fast drying [15]. However, there are also some disadvantages, such as easy aging and microcracks in daily use, which impinge on the beauty and service life of these products [16].

The service life of paint film can be prolonged by embedding a repair agent in the coating [17,18]. This specific implementation includes a liquid core fiber method and a microcapsule method [19]. Based on the application of microcapsule technology in composite materials, some progress has been made. Litina et al. [20] first applied the polymer microcapsules, including liquid sodium silicate, to the self-repair of industrial repair mortar, and the best self-healing additives were selected. Accordingly, it turned out that both the crack width and depth of the new composite cement-based repair material were reduced, and the permeability was restored. Njoku et al. [21] fabricated a novel pH-responsive permeability-switching polyurea-formaldehyde-coated 8-hydroxyquinoline microcapsule, which was used to prepare intelligent epoxy film for the permanent protection of Al-based alloys. The results indicated that the modified epoxy-based smart film has a good barrier and is active in improving the self-healing and corrosion inhibition performances. Wang et al. [22] synthesized fluorescent-labeled self-healing microcapsules (FLSM) by ultrasonic dispersion in-situ polymerization. Fluorescein sodium-labeled epoxy resin served as the restorative agent and UF resin as the cladding material. The results confirmed that FLSM can detect the position of microcracks and repair them and also indicates the width of microcracks on the cement surface. The above studies showed that the internal and external damage of the matrix material could be automatically repaired by mimicking the self-healing function of organisms and the participation of external environmental factors, to prolong the service life of the material. But it is worth noting that these studies focused on readily available commercial repair mortars, Al alloys and cement paste, and there are few reviews on the self-healing of waterborne wood paint films.

In our early work, epoxy resins laden with UF microcapsules were fabricated, and the effects of microcapsules and the coating process on gloss, color difference and the toughness of waterborne paint films for F. mandshurica veneers were studied [23]. As a common wood material, *Tilia europaea* has moderate hardness and a uniform and fine texture [24]. It is easy to process and possesses strong toughness, good corrosion resistance, wear resistance and resistance to crack deformation [25]. Nowadays, the demands of waterborne film-forming wood coatings are more and more extensive, so there is a need for a variety of wood substrates to meet the public aesthetic and to create application opportunities for self-healing wood products in a smart manner. Epoxy resin as a restorative agent needs to contain a hardener or a crosslinking agent and to be heated to achieve curing, which is not realistic for wood products, especially for furniture and floor products. Generally speaking, a waterborne primer is mainly used to fill pores and improve film thickness. On the other hand, the main function of a topcoat is to play the role of decoration and protection, such as keeping light and color, improving hardness and adhesion and leveling. Primer and topcoat have different functions, and their performances may be different. In this respect, the effect of microcapsules with different core-shell ratios on the performance of a waterborne primer for *Tilia europaea* was recently investigated [26]. Therefore, it is necessary to explore the presence of microcapsules on the properties of a waterborne topcoat on wood.

In this work, the safe and non-toxic water-based acrylic resin was used as the core material, and the hard and dense UF resin was used as the shell material to prepare microcapsules with seven different core-shell ratios. The microcapsules were added to the waterborne topcoat and spread on the *Tilia europaea* substrate to study the effect of the core-shell ratio and also the content of the microcapsules on the performance of the waterborne paint film. The waterborne acrylic resin with the same material as the paint base is selected as the core material to explore the effects of the addition of microcapsules on the optical properties, mechanical properties and liquid resistance of the waterborne topcoat. The repair agent can be cured at room temperature without introducing other media, which is conducive to interface bonding. In the future, the goal is to improve the repair rate of microcapsules. The results so obtained may serve as useful prerequisites in the preparation of self-healing waterborne wood coatings.

2. Materials and Methods

2.1. Experimental Materials

The materials required for the experiment are displayed in Table 1. The *Tilia europaea* with the size of 90 mm × 45 mm × 4 mm has been processed until its surface color was uniform, and its moisture content reached the local equilibrium, respectively 14.9%. The main components of waterborne topcoat were waterborne acrylic emulsion, polyurethane emulsion, additives and water.

Table 1. List of experimental materials.

Material	Molecular Formula	M_W (g/mol)	CAS No.	Concentration (%)	Producer
waterborne acrylic resin	-	-	9003-01-4	-	Dulux Paint Co., Ltd., Shanghai, China
urea	CH_4N_2O	60.06	57-13-6	99.9	Kunshan Southeast Chemical Materials Co., Ltd., Jiangsu, China
formaldehyde solution	CH_2O	30.03	50-00-0	37.0	
triethanolamine	$C_6H_{15}NO_3$	149.19	102-71-6	99.9	
citric acid monohydrate (CAM)	$C_6H_{10}O_8$	210.14	5949-29-1	99.9	
sodium dodecyl benzene sulfonate (SDBS)	$C_{18}H_{29}NaO_3S$	348.48	25155-30-0	99.9	
anhydrous ethanol	C_2H_6O	46.07	64-17-5	99.9	
n-octyl alcohol	$C_8H_{18}O$	130.23	117-87-5	99.9	Shanghai Aibi Chemical Reagent Co., Ltd., Shanghai, China
Tilia europaea	-	-	-	-	Shanghai Puhui industry and Trade Co., Ltd., Shanghai, China

2.2. Preparation of Microcapsules

Microcapsules with waterborne acrylic resin as the core material and UF resin as the shell material were prepared by in situ polymerization with the following values of the core-shell ratio as an independent variable: 0.42:1, 0.50:1, 0.58:1, 0.67:1, 0.75:1, 0.83:1 and 0.92:1 [27]. This paper mainly studied the effects of the core-shell ratio and the concentration of microcapsules on the properties of paint film. In later work, the stabilizer will be used to modify the microcapsules. The detailed compositions of the seven systems are shown in Table 2. To exemplify, the preparation process of microcapsules with a core-shell ratio of 0.42:1 was as follows:

Table 2. Material list of microcapsules with different core-shell ratios.

Urea (g)	37.0% Formaldehyde Solution (g)	Waterborne Acrylic Resin (g)	SDBS (g)	Distilled Water (g)	Core-Shell Ratio
40.0	54.0	25.0	1.8	193.0	0.42:1
40.0	54.0	30.0	2.2	231.6	0.50:1
40.0	54.0	35.0	2.6	271.2	0.58:1
40.0	54.0	40.0	3.0	308.8	0.67:1
40.0	54.0	45.0	3.4	348.4	0.75:1
40.0	54.0	50.0	3.8	386.0	0.83:1
40.0	54.0	55.0	4.2	425.6	0.92:1

The 40.0 g of urea and 54.0 g of formaldehyde solution were uniformly stirred with a magnetic stirrer. A corresponding amount of triethanolamine was added to adjust the pH to 8.0. The shell material was obtained after stirring the mixture for 70 min at 350 rpm and at a constant temperature of 75 °C. The emulsion of the core material was obtained by adding 25.0 g of waterborne acrylic resin into a mixture made of 1.8 g of sodium dodecyl benzene sulfonate (SDBS) and 193.0 g of distilled water (well-stirred previously) under vigorous stirring (1200 rpm) for 35 min at 60 °C. Then, the shell material solution was added into the core material emulsion, and the pH was adjusted to 2.0 by adding CAM under a stirring speed of 300 rpm for 2.5 h at 65 °C. The reaction mixture was kept at rest for 2 days at room temperature and then filtered, washed and dried to obtain the waterborne acrylic resin microcapsules with a core-shell ratio of 0.42:1.

2.3. Preparation of Waterborne Coatings

Seven types of microcapsules with different core-shell ratios (0.42:1, 0.50:1, 0.58:1, 0.67:1, 0.75:1, 0.83:1, 0.92:1) were prepared. Six kinds of coating films were prepared for each type of microcapsule. The mass fraction of microcapsules in the paint films was 0%, 5.0%, 10.0%, 15.0%, 20.0% and 25.0%, respectively. The materials required for the preparation of different core-shell ratio paint films are collected in Table 3. The microcapsules and waterborne coatings were mixed evenly and then spread on *Tilia europaea* substrate with a ZBQ tetrahedral preparator (Pushen Chemical Machinery Co., Ltd., Shanghai, China). Then the *Tilia europaea,* coated with water-based paint, was dried in a ventilated place for 25 min, then lightly polished with sandpaper until the paint film surface was smooth [28]. The above steps were repeated twice to obtain the paint film samples of about 60.0 microns thick required for further testing.

Table 3. Composition of self-healing waterborne topcoat.

Sample (#)	Microcapsule Concentration (%)	Mass of Microcapsule (g)	Mass of Waterborne Topcoat (g)	Mass of Self-Healing Waterborne Topcoat (g)
1	0	0	100.0	100.0
2	5.0	5.0	95.0	100.0
3	10.0	10.0	90.0	100.0
4	15.0	15.0	85.0	100.0
5	20.0	20.0	80.0	100.0
6	25.0	25.0	75.0	100.0

2.4. Testing and Characterization

The gloss of the paint film at 60° was tested by the WG-60G glossmeter (Shenzhen Baoan Sannuo Instrument Supplier, Shenzhen, China); the color difference of the paint film was tested by the WR-10 portable colorimeter (Shenzhen Baoan Sannuo Instrument Supplier, Shenzhen, China), and the chromaticity values of two points on the paint film were comparatively assessed. The chromaticity values of one point on the paint film were denoted as L_1, a_1, b_1, c_1 and H_1, and the chromaticity values of the second point were denoted as L_2, a_2, b_2, c_2 and H_2 [29]. The color difference (ΔE) was calculated according to

$$\Delta E = [(L_1 - L_2)^2 + (a_1 - a_2)^2 + (b_1 - b_2)^2]^{1/2} \quad (1)$$

The hardness of paint films was tested by QHQ pencil hardness tester (Shenzhen Baoan Sannuo Instrument Supplier, Shenzhen, China), according to the hardness sequence of 6B-6H. The tip of the pencil was ground flat; the paint film was fixed on the stage, and the pencil was inserted into the hardness tester, so that the pencil abutted on the paint film. The pencil hardness tester was moved slowly to observe the marks left behind by the pencil on the paint film. The hardness of the pencil with no scratching signs on the tested surface was considered the hardness of paint film.

The adhesive force was measured by a BYK cross-cut tester (Shenzhen Baoan Sannuo Instrument Supplier, Shenzhen, China). The paint film was drawn horizontally and vertically at the same place with the cross-cut tester, then pasted with adhesive tape. The adhesive force of the paint film was measured according to the peeling area of the paint film.

The impact resistance was tested by a QCJ-120 film impactor (Shenzhen Baoan Sannuo Instrument Supplier, Shenzhen, China). The paint film was placed at the bottom of the impactor, and the impactor impacted the paint film from progressively increasing heights. The height of the impactor at which microcracks appeared on the surface was considered the impact resistance of the paint film.

Sodium chloride, alcohol, detergent and red ink were used to test the liquid resistance of the paint film [30]. A filter paper soaked with these liquids taken individually was placed on the surface of the paint film and covered with a glass slide. One day later, the filter paper was removed, and the residual reagents on the surface of the paint film were wiped off. The change of the paint film was taken into account, and the color difference and gloss in the tested area were evaluated. According to the pollution of the paint film surface, the liquid resistance grade of paint film was determined, and the effects of these four solutions on paint film were compared. Liquid resistance grade 1 indicated that there was no obvious change on the surface of the paint film. Grade 2 indicated that there was slight discoloration or discontinuous marks on the surface of the paint film. Grade 3 indicated that there were obvious marks on the surface of the paint film. Grade 4 indicated that there were serious marks on the surface of the paint film, but the structure of the paint film had not been changed. Grade 5 indicated that the paint film was broken and the structure of the paint film was changed.

The surface morphology of prepared microcapsules and paint films was investigated by an EVO18 scanning electron microscope (Changzhou Jonah Electromechanical Technology Co., Ltd., Changzhou, China), while the chemical composition of the paint film was studied by a BFH-960 Fourier transform spectrometer (Guangzhou Biaoji Packaging Equipment Co., Ltd., Guangzhou, China). All the experiments were carried out four times, and the experimental error was within 5.0%.

3. Results and Discussion

3.1. Effect of Microcapsule on Optical Properties of Paint Films

The results of color difference of waterborne topcoats with different core-shell ratios are plotted in Figure 1. The color differences of paint films with different core-shell ratios were basically the same, except for the color difference of paint film with a 0.92:1 core-shell ratio, which was significantly greater than those corresponding to other ratios. However, as the microcapsule content increased, the color difference ascended at the same core-shell ratio. The color difference of the paint film with the microcapsule concentration of 0–10.0% was small.

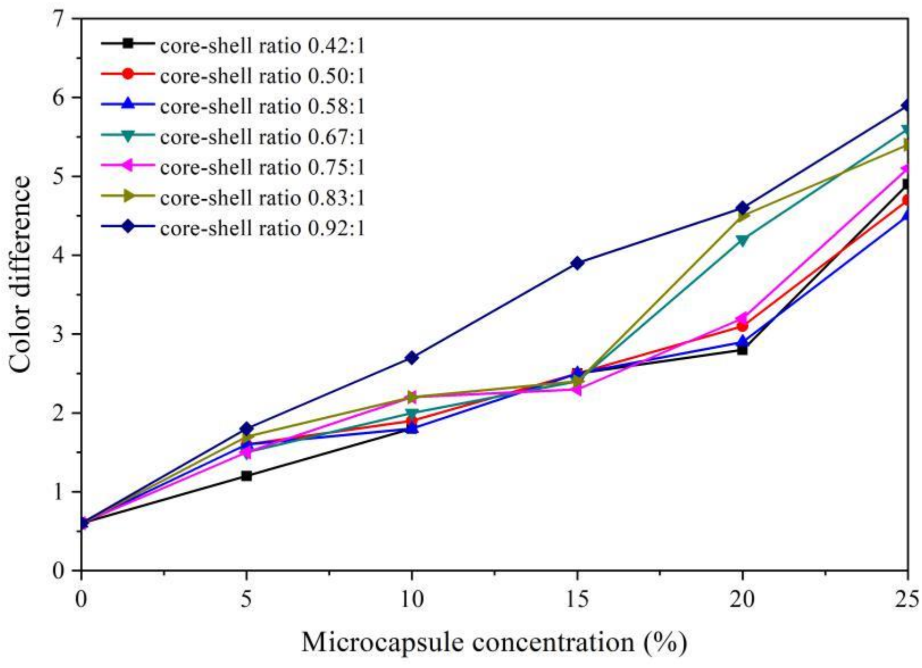

Figure 1. Effect of microcapsule concentration and core-shell ratio on the color differences of paint film.

The effect of the concentration of microcapsules with different core-shell ratios on the gloss of the paint film at 60° incident angle is shown in Figure 2. The paint film gloss was negatively correlated with the concentration of microcapsules. When the concentration increased from 0% to 5.0%, the gloss decreased steeply. When the concentration continued to increase, the gloss also showed a downward trend but with a lower decreasing rate. The reason was that the surface of paint film without microcapsules was smooth. After the addition of microcapsules, the number of particles increased, resulting in the enhancement of diffuse reflection on the surface of the paint film [31]. There was no significant difference in the overall gloss of the paint films with different core-shell ratios over the entire range of microcapsule concentration.

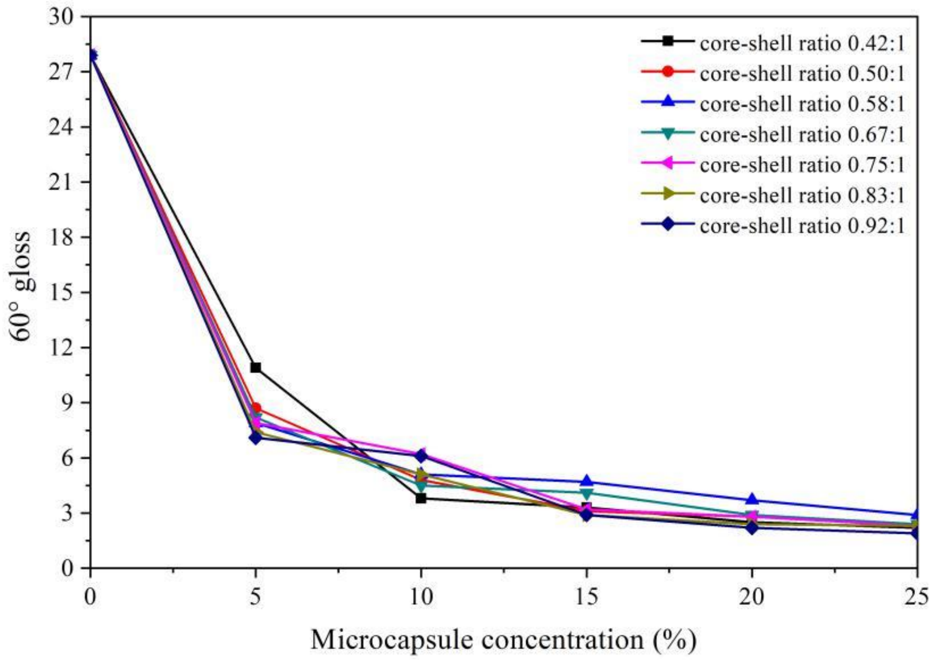

Figure 2. Effect of microcapsule concentration and core-shell ratio on gloss of paint film.

3.2. Effect of Microcapsule on Mechanical Properties of Paint Films

The hardness of paint films with different core-shell ratios of microcapsules is shown in Table 4. This quantity increased with the increase of microcapsule concentration in a certain range at the same core-shell ratio. The overall hardness of the paint films at the 0.42:1, 0.50:1, 0.58:1 and 0.67:1 core-shell ratio was higher than that of the last three core-shell ratios. At 0.75:1 and 0.92:1 core-shell ratios, as the microcapsule concentration reached 20.0–25.0%, the paint film hardness decreased. The main reason could have been that the microcapsules were agglomerated in the coatings, which reduces the interfacial bonding between the paint film and the microcapsules. Based on the results of gloss and color difference, the hardness of the paint film was better when the core-shell ratio was small and the microcapsule concentration ranged within 10.0%–15.0%.

Table 4. Effect of microcapsule concentration and core-shell ratio on the hardness of paint films.

Mass Fraction (%)	**Hardness**						
	0.42:1	**0.50:1**	**0.58:1**	**0.67:1**	**0.75:1**	**0.83:1**	**0.92:1**
0	HB	HB	HB	HB	HB	HB	HB
5.0	H	2H	H	2H	H	H	H
10.0	2H	3H	2H	3H	H	H	2H
15.0	2H	3H	3H	4H	2H	2H	2H
20.0	2H	3H	3H	4H	H	2H	H
25.0	2H	3H	3H	4H	H	2H	H

Table 5 shows the adhesion test results of waterborne topcoats with variable percentages of microcapsules deposited on *Tilia europaea*. The data proved that the adhesion of the paint film decreased with microcapsule concentration, which was due to the poor bonding interaction acting at the interface between the paint film and *Tilia europaea*. The adhesion was good enough at the core-shell ratio of 0.42:1, 0.50:1, 0.58:1 and 0.67:1. When the core-shell ratio was relatively larger, the adhesion became obviously poorer. This is because the high core-shell ratio of the microcapsules (0.75:1, 0.83:1, 0.92:1) induced the formation of microcapsule aggregates, which made spreading the topcoat onto substrate into a uniform film very difficult. Comparatively, when the microcapsule concentration was 0–10.0%, the adhesion of the paint film towards the substrate was the best.

Table 5. Effect of microcapsule concentration and core-shell ratio on the adhesion of the paint film onto the substrate.

Mass Fraction (%)	Adhesion (Level)						
	0.42:1	0.50:1	0.58:1	0.67:1	0.75:1	0.83:1	0.92:1
0	0	0	0	0	0	0	0
5.0	0	0	0	0	1	1	1
10.0	1	1	1	1	1	1	1
15.0	1	1	1	1	2	2	2
20.0	2	2	1	1	3	2	2
25.0	2	2	2	2	3	4	3

The impact resistance results of the paint films are displayed in Table 6. The data indicate that the paint films with 0.58:1 and 0.67:1 core-shell ratios of microcapsules had better impact resistance. At the same core-shell ratios, the impact resistance increased at first and then decreased with the increase in microcapsule content. The main reason for this behavior lies in the weak adherence of the film onto the substrate when the mass fraction of microcapsules is low and the ability of the paint film surface to maintain its integrity under external impact is reduced [32]. Practically, the best impact resistance data were obtained for the paint films characterized by a microcapsule concentration of 10.0–15.0% at the same core-shell ratios of 0.58:1 and 0.67:1.

Table 6. Effect of microcapsule concentration and core-shell ratio on the impact resistance of paint films.

Mass Fraction (%)	Impact Resistance (kg·cm)						
	0.42:1	0.50:1	0.58:1	0.67:1	0.75:1	0.83:1	0.92:1
0	5.0	5.0	5.0	5.0	5.0	5.0	5.0
5.0	7.0	8.0	10.0	9.0	7.0	8.0	8.0
10.0	9.0	12.0	15.0	14.0	9.0	10.0	12.0
15.0	10.0	12.0	12.0	15.0	9.0	13.0	12.0
20.0	10.0	10.0	12.0	11.0	9.0	12.0	12.0
25.0	8.0	10.0	9.0	11.0	13.0	12.0	10.0

Based on the fact that the best data of hardness, adhesion and impact resistance have been obtained for the paint films with core-shell ratios of 0.42:1–0.67:1, irrespective of the mass fraction of microcapsules, the systems with the same compositional characteristics have been tested via elongation at break. It can be seen from Figure 3 that, at the same core-shell ratio, with the growing concentration of microcapsule, the elongation at break of the paint film first increased and then decreased, but the overall change range was small. However, the best data of the elongation at break were obtained for the paint films with a core-shell ratio of 0.58:1 and a microcapsule concentration of 10.0–15.0%.

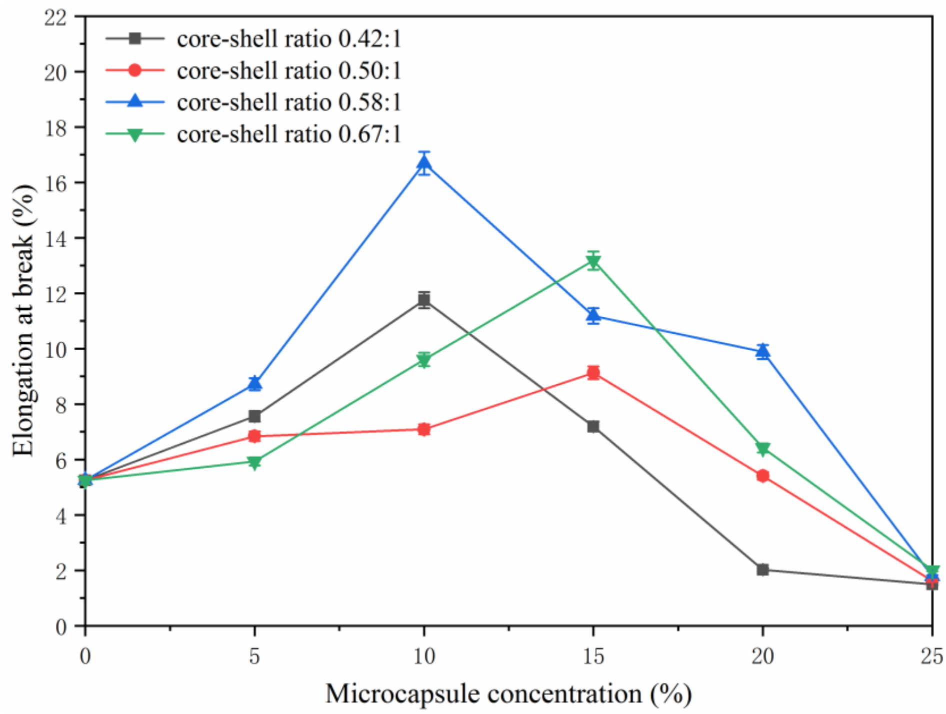

Figure 3. Effect of microcapsule concentration and core-shell ratio on elongation at break of paint film.

3.3. Effect of Microcapsule on the Liquid Resistance of Paint Films

The color difference values obtained after liquid resistance tests performed on paint films shown in Table 7 were quite small, except for the red ink test. In this particular case, the color difference of the paint film markedly increased when the mass fraction of microcapsules reached 25.0%. The color difference changed more greatly under the larger core-shell ratio conditions. On the other hand, the paint film gloss essentially had no change before and after the four kinds of liquid resistance experiments (see Table 8). Overall, the gloss decreased slightly after the red ink by comparison with the gloss measured after the other three types of liquid resistance tests. The results of paint film liquid resistance level were determined and are displayed in Table 9. In the case of the 0.42:1 to 0.67:1 core-shell ratio, the liquid resistance level of the paint film to NaCl, ethanol and detergent was level 1 without any mark. When the core-shell ratio was above 0.75:1 and the microcapsule concentration was high, the liquid resistance level of the paint film to these three liquids was poor. With the increase in microcapsule content, the liquid resistance level of the paint film to NaCl, ethanol and detergent was almost the same, while the liquid resistance to red ink gradually deteriorated. Generally, when the core-shell ratio was small and the microcapsule concentration was 0–15.0%, the liquid resistance of the paint film was better.

Table 7. Effect of microcapsule concentration and core-shell ratio on the color difference of painted surfaces after exposure to different liquids.

Core-Shell Ratio	Mass Fraction (%)	Color Difference			
		NaCl	Ethanol	Detergent	Red Ink
0.42:1	0	1.2	0.3	1.1	1.7
	5.0	1.0	0.9	0.8	2.4
	10.0	0.5	0.9	1.1	2.4
	15.0	1.0	0.9	0.4	2.4
	20.0	0.5	0.3	0.5	3.3
	25.0	0.4	0.8	0.5	16.9
0.50:1	0	1.2	0.3	1.1	1.7
	5.0	1.0	0.5	0.5	1.8
	10.0	0.8	0.5	1.0	2.1
	15.0	0.8	0.9	0.4	2.0
	20.0	0.4	0.6	1.0	2.3
	25.0	0.8	1.1	0.4	4.2
0.58:1	0	1.2	0.3	1.1	1.7
	5.0	0.9	1.0	1.0	2.7
	10.0	0.7	0.8	0.7	3.1
	15.0	1.0	0.8	0.8	3.4
	20.0	1.1	0.8	1.1	3.4
	25.0	0.9	0.5	1.0	6.0
0.67:1	0	1.2	0.3	1.1	1.7
	5.0	0.9	1.1	0.8	3.8
	10.0	1.1	1.1	0.9	3.4
	15.0	0.8	0.5	0.9	2.5
	20.0	1.1	1.0	0.6	3.1
	25.0	1.1	1.1	0.7	4.9
0.75:1	0	1.2	0.3	1.1	1.7
	5.0	0.6	1.1	0.8	3.4
	10.0	0.7	1.0	0.9	2.8
	15.0	1.1	1.7	0.3	4.4
	20.0	0.8	2.3	1.0	4.8
	25.0	1.1	3.9	0.8	10.7
0.83:1	0	1.2	0.3	1.1	1.7
	5.0	0.8	1.0	0.8	2.1
	10.0	0.9	0.7	0.5	2.0
	15.0	1.1	1.1	0.9	2.0
	20.0	2.0	1.7	0.5	8.4
	25.0	2.1	2.9	0.8	7.7
0.92:1	0	1.2	0.3	1.1	1.7
	5.0	0.8	0.8	0.7	2.8
	10.0	1.1	0.4	1.1	2.9
	15.0	0.3	1.2	1.0	2.3
	20.0	1.8	2.2	0.4	14.4
	25.0	1.3	2.3	2.7	18.2

Table 8. Effect of microcapsule concentration and core-shell ratio on the gloss of painted surfaces after exposure to different liquids.

Core-Shell Ratio	Mass Fraction (%)	Gloss (%)			
		NaCl	Ethanol	Detergent	Red Ink
0.42:1	0	27.3	27.9	27.9	25.6
	5.0	10.4	10.6	10.4	9.2
	10.0	3.9	3.7	3.7	3.2
	15.0	3.2	3.3	3.2	3.3
	20.0	2.8	2.4	2.3	2.4
	25.0	2.1	2.1	2.3	1.7
0.50:1	0	27.3	27.9	27.9	25.6
	5.0	8.5	8.7	8.5	8.8
	10.0	4.4	4.7	4.5	4.1
	15.0	3.0	3.0	3.1	2.9
	20.0	2.5	2.5	2.6	2.2
	25.0	2.2	2.3	2.4	2.0
0.58:1	0	27.3	27.9	27.9	25.6
	5.0	7.5	7.5	7.6	6.8
	10.0	5.0	4.9	4.8	4.7
	15.0	4.8	4.7	4.5	4.1
	20.0	3.4	3.4	3.5	2.8
	25.0	2.6	2.5	2.9	2.3
0.67:1	0	27.3	27.9	27.9	25.6
	5.0	8.4	8.9	8.8	8.1
	10.0	4.5	4.7	4.3	3.9
	15.0	4.0	4.0	3.9	3.6
	20.0	2.5	2.5	2.7	2.4
	25.0	2.2	2.2	2.4	2.1
0.75:1	0	27.3	27.9	27.9	25.6
	5.0	7.5	8.0	8.1	7.8
	10.0	6.2	6.1	6.2	5.3
	15.0	3.0	3.0	3.1	2.8
	20.0	2.4	2.4	2.5	2.3
	25.0	2.1	2.4	2.2	1.8
0.83:1	0	27.3	27.9	27.9	25.6
	5.0	7.2	7.2	7.5	7.5
	10.0	5.0	4.8	4.8	3.9
	15.0	2.3	2.3	2.5	2.2
	20.0	2.2	2.1	2.3	1.8
	25.0	2.0	2.1	2.1	1.8
0.92:1	0	27.3	27.9	27.9	25.6
	5.0	9.5	9.6	9.2	9.0
	10.0	5.9	5.7	5.7	5.1
	15.0	2.6	2.8	2.9	2.6
	20.0	2.2	2.2	2.3	1.6
	25.0	1.9	2.1	1.8	1.7

Table 9. Effect of microcapsule concentration and core-shell ratio on liquid resistance level.

Core-Shell Ratio	Mass Fraction (%)	Liquid Resistance Level (Level)			
		NaCl	Ethanol	Detergent	Red Ink
0.42:1	0	1	1	1	1
	5.0	1	1	1	2
	10.0	1	1	1	2
	15.0	1	1	1	2
	20.0	1	1	1	3
	25.0	1	1	1	3
0.50:1	0	1	1	1	1
	5.0	1	1	1	1
	10.0	1	1	1	2
	15.0	1	1	1	2
	20.0	1	1	1	2
	25.0	1	1	1	3
0.58:1	0	1	1	1	1
	5.0	1	1	1	2
	10.0	1	1	1	3
	15.0	1	1	1	3
	20.0	1	1	1	3
	25.0	1	1	1	3
0.67:1	0	1	1	1	1
	5.0	1	1	1	3
	10.0	1	1	1	3
	15.0	1	1	1	2
	20.0	1	1	1	3
	25.0	1	1	1	3
0.75:1	0	1	1	1	1
	5.0	1	1	1	3
	10.0	1	1	1	2
	15.0	1	1	1	3
	20.0	1	2	1	3
	25.0	1	2	1	3
0.83:1	0	1	1	1	1
	5.0	1	1	1	2
	10.0	1	1	1	2
	15.0	1	1	1	2
	20.0	2	1	1	3
	25.0	2	2	1	3
0.92:1	0	1	1	1	1
	5.0	1	1	1	2
	10.0	1	1	1	2
	15.0	1	1	1	2
	20.0	1	2	1	3
	25.0	1	2	2	3

3.4. Morphology Characterization and Chemical Composition Analysis

According to the above results of the optical properties, mechanical properties and liquid resistance of the paint films, the paint films with the microcapsules of 0.58:1 core-shell ratio have the best performance. The morphology of microcapsules with a core-shell ratio of 0.58:1 revealed a spherical shape and a relatively uniform particle size of 5 microns, as can be seen in Figure 4.

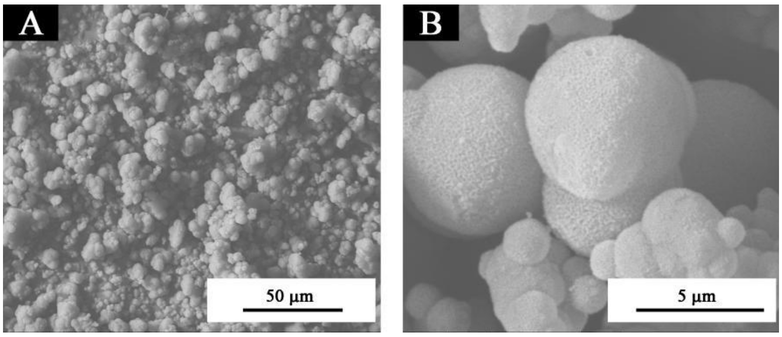

Figure 4. SEM of microcapsules of with a 0.58:1 core-shell ratio: (**A**) low and (**B**) high magnification.

SEM images of the paint film with different microcapsule concentrations and the same core-shell ratio of 0.58:1 is inserted in Figure 5. The surface of the paint film without microcapsules was smooth (Figure 5A). Instead, at low particle concentration, the film appearance indicates microcapsules are evenly distributed, but, at a high particle fraction of 25.0%, an aggregation phenomenon tends to prevail on the surface of the investigated paint films (Figure 5B–D).

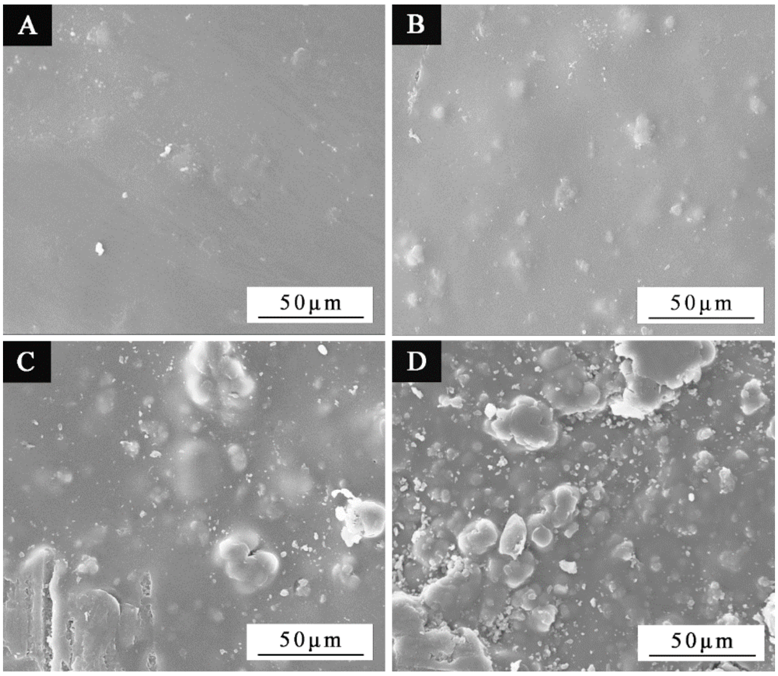

Figure 5. SEM of paint film with different concentrations of microcapsules (core-shell ratio = 0.58:1): (**A**) 0, (**B**) 5.0%, (**C**) 10.0%, (**D**) 25.0%.

Figure 6 shows the FTIR spectra of the paint films with microcapsules of different concentrations and a core-shell ratio of 0.58:1. There was O–H and N–H antisymmetric tensile vibration and symmetric tensile vibration at 3360 cm^{-1} [33]. The stretching vibration absorption peak of saturated C–H was mainly near 2929 cm^{-1} and 2865 cm^{-1} [27]. The double peak stretching vibration peak of the C–N secondary amide bond was near 1639 cm^{-1} and 1447 cm^{-1}, and the bending vibration absorption peak of N–CO–N was at wave number 646 cm^{-1}, indicating that the wall material of microcapsule was urea formaldehyde resin. The 1730 cm^{-1} was the characteristic peak of C=O of water-based acrylic resin. As the concentration changed, the peaks did not disappear, indicating that there was no difference in paint film composition with different microcapsule concentrations.

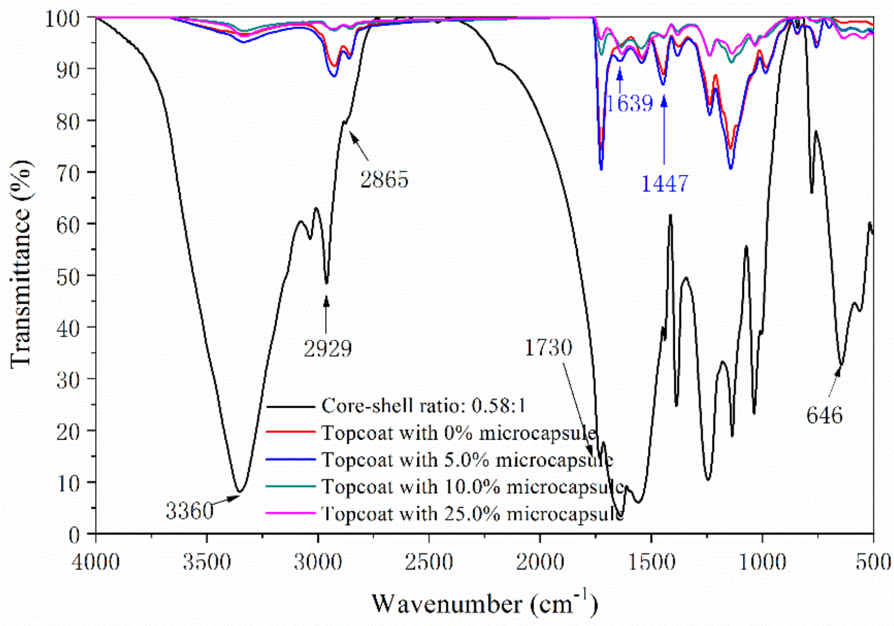

Figure 6. FTIR spectra of paint films with different concentrations of microcapsules (core-shell ratio = 0.58:1).

4. Conclusions

The UF-coated waterborne acrylic resin microcapsule with the different core-shell ratios and the same concentration had little effect on the overall color difference and gloss of the paint film. When the core-shell ratio was 0.58:1–0.67:1 and the microcapsule concentration was 10.0–15.0%, the hardness of the paint films was 2H–4H and the impact resistance was 12.0–15.0 kg·cm. The adhesion of the paint films was high at the core-shell ratio of 0.42:1–0.67:1. When the core-shell ratio of microcapsules was 0.58:1 and the microcapsule concentration was 10.0%, the color difference of the paint film was 1.8, the gloss was 5.1, the hardness was 2H, the adhesion was grade 1, the impact resistance was 15.0 kg·cm, the elongation at break of the paint film was 16.7%, and the resistance to NaCl, ethanol and detergent was grade 1; at this time, the comprehensive performance of waterborne paint film on *Tilia europaea* surface was better. The results provided the technical assistance for the development of self-healing waterborne wood coatings.

Author Contributions: Conceptualization, methodology, validation, resources, data management, supervision, X.Y.; Formal analysis, investigation, writing-review and editing, W.Z., Investigation and writing-review, L.W. and X.Q. All authors have read and agreed to the published version of the manuscript.

Funding: This project was partly supported by the Natural Science Foundation of Jiangsu Province (BK20201386).

Institutional Review Board Statement: Not applicable.

Informed Consent Statement: Not applicable.

Data Availability Statement: Not applicable.

Conflicts of Interest: The authors declare that there is no conflict of interest.

References

1. Wu, Q.; Zhao, B.Z.; Liu, S.W.; Yu, S.T.; Huang, L.; Ragauskas, A.J. From cellulose to 1,2,4-benzenetriol via catalytic degradation over a wood-based activated carbon catalyst. *Catal. Sci. Technol.* **2020**, *10*, 3423–3432. [CrossRef]
2. Xiong, X.Q.; Bao, Y.L.; Guo, W.J.; Fang, L.; Wu, Z.H. Preparation and application of high performance corn starch glue in straw decorative panel. *Wood Fiber Sci.* **2018**, *50*, 88–95.

3. Xu, W.; Fang, X.Y.; Han, J.T.; Wu, Z.H.; Zhang, J.L. Effect of coating thickness on sound absorption property of four wood species commonly used for piano soundboards. *Wood Fiber Sci.* **2020**, *52*, 28–43. [CrossRef]
4. Ozgenc, O.; Durmaz, S.; Sahin, S.; Boyaci, I.H. Evaluation of the weathering resistance of waterborne acrylic- and alkyd-based coatings containing HALS, UV absorber, and bark extracts on wood surfaces. *J. Coat. Technol. Res.* **2020**, *17*, 461–475. [CrossRef]
5. Chen, J.Y.; Wang, Y.J.; Cao, J.Z.; Wang, W. Improved water repellency and dimensional stability of wood via impregnation with an epoxidized linseed oil and carnauba wax complex emulsion. *Forests* **2020**, *11*, 271. [CrossRef]
6. Chen, W.C.; Tejado, A.; Alam, M.N.; van de Ven, T.G.M. Hydrophobic cellulose: A material that expands upon drying. *Cellulose* **2015**, *22*, 2749–2754. [CrossRef]
7. Liu, M.; Xu, G.L.; Wang, J.A.; Tu, X.W.; Liu, X.Y.; Wu, Z.H.; Lv, J.F.; Xu, W. Effects of shellac treatment on wood hygroscopicity, dimensional stability and thermostability. *Coatings* **2020**, *10*, 881. [CrossRef]
8. Xiong, X.Q.; Yuan, Y.Y.; Niu, Y.T.; Zhang, L.T. Development of a cornstarch adhesive for laminated veneer lumber bonding for use in engineered wood flooring. *Int. J. Adhes. Adhes.* **2020**, *98*, 102534.
9. Torun, S.B.; Cavdar, A.D.; Ozdemir, T. The synergistic effect of intumescent coating containing titanium dioxide and antimony trioxide onto spruce and alder wood species. *J. Build. Eng.* **2020**, *31*, 101407. [CrossRef]
10. Cheng, L.S.; Ren, S.B.; Lu, X.N. Application of eco-friendly waterborne polyurethane composite coating incorporated with nano cellulose crystalline and silver nano particles on wood antibacterial board. *Polymers* **2020**, *12*, 407. [CrossRef]
11. Zhang, T.X.; Ting, G.; Wu, Z.H.; Sun, T. Reinforced strength evaluation of binding material for the restoration of Chinese ancient lacquer furniture. *BioResources* **2019**, *14*, 7182–7192.
12. Liu, Q.Q.; Gao, D.; Xu, W. Influence of the bottom color modification and material color modification process on the performance of modified Poplar. *Coatings* **2021**, *11*, 660. [CrossRef]
13. Wu, S.S.; Tao, X.; Xu, W. Thermal conductivity of Poplar wood veneer impregnated with graphene/polyvinyl alcohol. *Forests* **2021**, *12*, 777. [CrossRef]
14. Kafle, B.; Gieri, P.; Kookhaee, H.; Tesema, T.E.; Haq, S.; Manjavacas, A.; Habteyes, T.G. Robust charge transfer plasmons in metallic particle-film systems. *ACS Photonics* **2018**, *5*, 4022–4029. [CrossRef]
15. Yu, Y.; Li, A.Q.; Yan, K.Y.; Ramaswamy, H.S.; Zhu, S.M.; Li, H.H. High-pressure densification and hydrophobic coating for enhancing the mechanical properties and dimensional stability of soft poplar wood boards. *J. Wood. Sci.* **2020**, *66*, 45. [CrossRef]
16. Chen, K.L.; Zhou, J.L.; Che, X.G.; Zhao, R.Y.; Gao, Q. One-step synthesis of core shell cellulose-silica/n-octadecane microcapsules and their application in waterborne self-healing multiple protective fabric coatings. *J. Colloid Interf. Sci.* **2020**, *566*, 401–410. [CrossRef]
17. Kardar, P. The effect of polyurethane-isophorone microcapsules on self-healing properties of an automotive clearcoat. *Pigm. Resin Technol.* **2016**, *45*, 73–78. [CrossRef]
18. Feng, Y.Y.; Cui, Y.X.; Zhang, M.J.; Li, M.L.; Li, H.Y. Preparation of tung oil-loaded PU/PANI microcapsules and synergetic anti-corrosion properties of self-healing epoxy coatings. *Macromol. Mater. Eng.* **2020**, *206*, 2000581. [CrossRef]
19. Li, J.Y.; Shi, H.W.; Liu, F.C.; Han, E.H. Self-healing epoxy coating based on tung oil-containing microcapsules for corrosion protection. *Prog. Org. Coat.* **2021**, *156*, 106236. [CrossRef]
20. Litina, C.; Al-Tabbaa, A. First generation microcapsule-based self-healing cementitious construction repair materials. *Constr. Build. Mater.* **2020**, *255*, 119389. [CrossRef]
21. Njoku, C.N.; Bai, W.C.; Arukalam, I.O.; Yang, L.H.; Hou, B.R.; Njoku, D.I.; Li, Y. Epoxy-based smart coating with self-repairing polyurea-formaldehyde microcapsules for anticorrosion protection of aluminum alloy AA2024. *J. Coat. Technol. Res.* **2020**, *17*, 797–813. [CrossRef]
22. Wang, X.G.; Chen, Z.F.; Xu, W.; Wang, X.J. Fluorescence labelling and self-healing microcapsules for detection and repair of surface microcracks in cement matrix. *Compos. Part B-Eng.* **2020**, *184*, 107744. [CrossRef]
23. Yan, X.X.; Qian, X.Y.; Chang, Y.J. Preparation and characterization of urea formaldehyde @ epoxy resin microcapsule on waterborne wood coatings. *Coatings* **2019**, *9*, 475. [CrossRef]
24. Gao, P.Z.; Wu, M.J.; Li, B.J.; Liu, Y.L. Structure characterization and oxidation mechanism study of porous biomorphic carbon template derived from Basswood. *Mater. Res. Bull.* **2009**, *44*, 644–648. [CrossRef]
25. Qian, J.M.; Wang, J.P.; Jin, Z.H. Preparation of biomorphic SiC-ceramics by the reactive infiltration on of Si into carbon template derived from basswood. *Rare Metal Mat. Eng.* **2004**, *33*, 1065–1068.
26. Yan, X.X.; Wang, L.; Qian, X.Y. Effect of microcapsules with different core-wall ratios on properties of waterborne primer coating for European Linden. *Coatings* **2020**, *10*, 826. [CrossRef]
27. Yan, X.X.; Tao, Y.; Qian, X.Y. Preparation and optimization of waterborne acrylic core microcapsules for waterborne wood coatings and comparison with epoxy resin core. *Polymers* **2020**, *12*, 2366. [CrossRef]
28. Liu, Q.Q.; Gao, D.; Xu, W. Effect of sanding processes on the surface properties of modified Poplar coated by primer compared with Mahogany. *Coatings* **2020**, *10*, 856. [CrossRef]
29. Li, R.R.; He, C.J.; Chen, Y.J.; Wang, X.D. Effects of laser parameters on the width of color change area of poplar wood surface during a single irradiation. *Eur. J. Wood Wood Prod.* **2021**, *79*, 1109–1116. [CrossRef]
30. GB/T 4893.1-2005. *Furniture—Assessment of Surface Resistance to Cold Liquids*; Standardization Administration of the People's Republic of China: Beijing, China, 2005; pp. 1–5. (In Chinese)

31. Ataei, S.; Khorasani, S.N.; Torkaman, R.; Neisiany, R.E.; Koochaki, M.S. Self-healing performance of an epoxy coating containing microencapsulated alkyd resin based on coconut oil. *Prog. Org. Coat.* **2018**, *120*, 160–166. [CrossRef]
32. Mirabedini, S.M.; Kiamanesh, A. The effect of micro and nano-sized particles on mechanical and adhesion properties of a clear polyester powder coating. *Prog. Org. Coat.* **2013**, *76*, 1625–1632. [CrossRef]
33. Wang, Y.; Bai, W.Y.; Cui, Z.C. Fourier transform infrared spectroscopic study of pesticide microcapsules influenced by formaldehyde to urea ratio. *Spectrosc. Left.* **2015**, *48*, 259–264. [CrossRef]